the FPC is proven inadequate to represent mid-IR VCD, the LMO will *not* be a useful alternative for stereochemical analysis.

Finally, it should be clear that these substituted allenes form a class of molecules with stereoelectronic effects of interest for study with VCD. Yet, at the same time, they are not ammenable to the more quantitatively reliable, large-basis-set type calculations of Stephens and co-workers.[18] Thus the applicability of simpler, though deficient, VCD models remains a viable problem for future research. Its solution will be needed to attain extensive stereochemical utility for VCD with even these relatively small molecules.

Acknowledgment. This work was supported by a grant from the National Science Foundation (CHE84-12087) for which we are most grateful. We also thank Prof. P. L. Polavarapu for giving us a copy of his LMO-VCD program and Dr. A. Annamalai for assistance in programming and critical comments on this manuscript.

Experimental and Theoretical Study of the Structures and Optical Rotations of Chiral Bicyclic Ortho Esters

A. E. Wroblewski,[†,1] J. Applequist,[‡] A. Takaya,[‡,§] R. Honzatko,[‡,§] S.-S. Kim,[†,§] R. A. Jacobson,[†,§] B. H. Reitsma,[†,§] E. S. Yeung,[†,§] and J. G. Verkade*[,†]

Contribution from the Department of Chemistry, Department of Biochemistry and Biophysics, and Ames Laboratory of the DOE,[2] Iowa State University, Ames, Iowa 50011.
Received August 17, 1987

Abstract: Syntheses are described for three rigid (-)-1-R-2,7,8-trioxabicyclo[3.2.1]octanes (R = H, **1**; R = Me, **2**; R = Ph, **3**) in high enantiomeric purity. The crystal and molecular structure of (-)-**3** was determined by X-ray means. A crystal of (-)-**3** grown from Et_2O-n-C_6H_{14} belonged to the space group $P2_1$ having cell constants a = 7.8520 (9), b = 10.493 (1), and c = 6.1048 (6) Å and β = 107.02 (1)°. The cell volume was 481.35 (9) Å^3 with 2 molecules per unit cell. The final conventional residual index was 0.0612. From the crystallographic data, four refined structural models of **3** were generated, which differed only in their degree of geometric optimization. Whereas model 1 is unrestrained, models 2-4 are increasingly restrained to ideal geometry in order to correct the systematically short bonds associated with an unrestrained refinement. Molar rotations were calculated from classical dipole interaction theory with the structural parameters from the four models of **3** and atom polarizabilities derived earlier. The calculated molar rotations for **3** were correct in sign and insensitive to rotations of the phenyl group about the C-C bond. The differences between the calculated values and the experimental rotation decreased to within a factor of 4 concomitantly with the increased level of geometric optimization of the models. The difference between the theoretical and experimental values is attributable to small uncertainties in atom coordinates and atom polarizabilities. Similar results were obtained for **1** and **2** with the structural models obtained for **3**. The identical signs and similar magnitudes of rotations for **1**-**3** appear to stem primarily from the chiral gauche arrangement of the butane fragment.

Ortho esters **1**-**3** are nearly rigid chiral molecules derived from optically active 1,2,4-butanetriol. The lack of conformational freedom in these molecules confers on them special theoretical

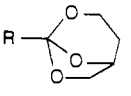

1, R=H
2, R=Me
3, R=Ph

interest, because it is possible to make meaningful theoretical calculations of their optical activity without resorting to rather uncertain conformational averaging. These molecules are also amenable to the classical dipole interaction theory,[3] which has been applied successfully to a variety of optically active molecules, ranging from the simplest known case of CHFClBr[3-5] to complex helical polypeptides.[6] In the simplest molecular model treated by this theory, the atoms are regarded as isotropic units that interact with each other only by way of the fields of their induced electric dipole moments in the field of a light wave. This approach works well for essentially saturated molecules, presumably because the high degree of electron localization implicit in the model is most nearly valid for such molecules. We employ this approach for the ortho esters **1**-**3**, since the chiral bicyclic moiety in each is saturated. Moreover, these esters can be synthesized in enantiomerically pure form for reliable optical rotation measurements, and **3** gave crystals suitable for X-ray diffraction determination of the required structural parameters.

To predict the optical rotation at the sodium D line (5893 Å), the theory requires the polarizabilities and coordinates of all atoms in the molecule. The atom polarizabilities have been obtained semiempirically from observed molecular polarizabilities of simple compounds at the sodium D line.[7] In most previous studies of this type, reasonably accurate atom coordinates were generated from bond lengths and bond angles obtained from various sources. Compounds **1**-**3** must be approached differently because their bicyclic configuration is strained, rendering accurate predictions of their structures from "standard" bond lengths and bond angles unfeasible. The approach adopted in this study was to determine the structure of a single crystal of a pure enantiomer of one of the ortho esters (**3**) by X-ray diffraction and then to utilize the coordinates so found for the bicyclic moiety in calculating the

[†] Department of Chemistry.
[‡] Department of Biochemistry and Biophysics.
[§] Ames Laboratory of the DOE.

(1) On leave from the Institute of Organic Chemistry, Technical University, Lodz, Poland.
(2) Ames Laboratory is operated for the U.S. Department of Energy by Iowa State University under Contract No. W-7 405-Eng-82.
(3) Applequist, J. *Acc. Chem. Res.* **1977**, *10*, 79.
(4) Canceill, J.; Lacombe, L.; Collet, A. *J. Am. Chem. Soc.* **1985**, *107*, 6993.
(5) Wilen, S. H.; Bunding, K. A.; Kascheres, C. M.; Wieder, M. J. *J. Am. Chem. Soc.* **1985**, *107*, 6997.
(6) Applequist, J. *Am. Sci.* **1987**, *75*, 58.
(7) Applequist, J.; Carl, J. R.; Fung, K.-K. *J. Am. Chem. Soc.* **1972**, *94*, 2952.

0002-7863/88/1510-4144$01.50/0

optical rotations of the remaining members of the series. Because of the high sensitivity of the calculated rotations to the atomic coordinates, this approach is subject to the experimental uncertainties inherent in the X-ray diffraction technique. Thus, we explore here some restrained refinement procedures to reduce the effect of these uncertainties on the calculated molar rotations.

The sign of the optical rotation, even at a single wavelength, contains sufficient information to establish the absolute configuration of the molecule. A major objective of any theory of optical activity should be to establish the relationship between the sign and the configuration. The present study shows that the dipole interaction theory accomplishes this for the esters **1–3**, though it also reveals a potential hazard in establishing this connection for molecules wherein interactions of high order among atoms are significant.

Experimental Section

Solvents used for the syntheses of **1–3** were distilled prior to use from sodium benzophenone ketyl. For column chromatography Davisil 62 silica gel (Davison Chemicals) was employed. Melting points were taken on a Thomas Hoover capillary melting point apparatus and are uncorrected. Proton and carbon-13 NMR spectra were measured on a Nicolet NT-300 NMR spectrometer in deuteriochloroform, and chemical shifts are reported in parts per million downfield from tetramethylsilane by use of chloroform (7.26 ppm) and deuteriochloroform (71.0 ppm) resonances, respectively, as secondary standards. Phosphorus-31 NMR spectra were taken on a Bruker WM-300 spectrometer. Optical rotations were measured on a Perkin-Elmer 141 polarimeter. The specific rotation $[\alpha]$ was converted to the intrinsic molar rotation $[m]$ by $[m] = [\alpha](M_r/100)[3/(n^2 + 2)]$, where M_r is the molecular weight of the solute and n is the refractive index of the solvent, taken as 1.4893 for toluene. Solutions for the optical activity measurements were prepared in a glovebag under nitrogen. Hydrogen chloride was dried by passage through P_4O_{10}.

Dimethyl (*S*)-(−)-Malate. Although this compound has been prepared previously,[8,9] the following method is convenient, proceeds in high yield, and gives a product of high purity. Dry hydrogen chloride was slowly passed through a solution of L-malic acid (47.3 g, 0.350 mol) in methanol (200 mL) for 5 min. The reaction mixture was left at room temperature overnight. Volatile materials were evaporated, and the residue was distilled to give the diester (39.5 g, 70%) as a colorless oil [bp 74 °C (1.5 mmHg)]. The residue was dissolved in methanol (70 mL), and again dry hydrogen chloride was passed through the solution for 5 min. After the mixture was left overnight at room temperature, and the lower boiling materials were evaporated, additional diester (16.0 g, total 98% yield) was collected [bp 74–76 °C (1.5 mmHg)]. Redistillation of the product through a short Vigreux column gave dimethyl (*S*)-(−)-malate (51.0 g, 91% yield) as a colorless oil: ^{1}H NMR ($CDCl_3$) δ 2.75–2.91 (2 H, AB part of ABX system, J_{AB} = 16.4 Hz, CH_2), 3.25–3.35 (1 H, br s, OH), 3.70 and 3.80 (6 H, 2 s, CH_3OOC), 4.45–4.53 (1 H, m, CH). The optical rotation of this distillate [$[\alpha]^{25}_D$ −8.4° (neat)] exceeded literature values [lit.[8] $[\alpha]^{25}_D$ −7.57°, lit.[9] $[\alpha]^{25}_D$ −7.0° (neat)].

(*S*)-(−)-1,2,4-Butanetriol. This compound was obtained by literature procedures from the above ester[10] in 47% yield [$[\alpha]^{25}_D$ −28.7° (*c* 7.62, absolute EtOH)] and from L-malic acid[11] in 89% yield [$[\alpha]^{25}_D$ −27.4° (*c* 2.45, MeOH) [lit.[12] $[\alpha]^{25}_D$ −29° (*c* 1.035, MeOH)]].

2,7,8-Trioxabicyclo[3.2.1]octanes 1–3. A general procedure was followed. 1,2,4-Butanetriol (5.3 g, 50 mmol) was weighed into a 250-mL flask. The flask was evacuated, warmed with a heat gun, allowed to cool to room temperature, and flushed with nitrogen. Tetrahydrofuran (ca. 200 mL) was distilled into the flask. The appropriate trimethyl ortho ester (50 mmol) was then injected into the flask through a rubber septum followed by a few bubbles of dry HCl. After the reaction mixture was stirred at room temperature for 6–8 h, powdered anhydrous potassium carbonate (1 g) was added, and the fine suspension was stirred overnight. Removal of THF under vacuum and distillation in vacuo afforded the crude products, which were further purified on the silica gel column with chloroform–triethylamine (200:1, v/v) to give the following.

(±)-**1**: 2.17 g (37% yield); bp 63–65 °C (8 mmHg) [lit.[13] mp 58 °C (8 mmHg)]; mp 48–49 °C (lit.[14] mp 47–49 °C); ^{13}C NMR δ 28.71 (C4), 57.21 (C3), 67.77 (C6), 71.38 (C5), 111.52 (C1).

(−)-**1**: 13.5% yield; bp 63 °C (7 mmHg); colorless oil that solidified on cooling; $[\alpha]^{27}_D$ −175.8° (*c* 9.32, toluene).

(±)-**2**: 4.81 g (74% yield); bp 53–54 °C (7 mmHg); colorless liquid; ^{13}C NMR δ 22.00 (CH_3), 27.96 (C4), 58.46 (C3), 68.78 (C6), 72.91 (C5), 118.97 (C1).

(−)-**2**: 63% yield; bp 59 °C (12 mmHg); colorless liquid; $[\alpha]^{22}_D$ −139.2° (*c* 9.71, toluene).

(±)-**3**: 3.33 g (35% yield); bp 105–107 °C (0.1 mmHg); mp 61.0–61.5 °C (from ether–hexane); ^{13}C NMR δ 27.84 (C4), 58.95 (C3), 69.04 (C6), 73.32 (C5), 118.03 (C1), 127.75, 125.63, 129.05, 132.62 (aromatic carbons).

(−)-**3**: 39% yield; bp 100–105 °C (0.08 mmHg); mp 59.5–60.5 °C (from ether–hexane); $[\alpha]^{23}_D$ −88.9° (*c* 9.68, toluene).

X-ray Structure Determination of (±)-3. Parameters of the unit cell and information relevant to data collection appear in Table I. The unit cell dimensions and lattice symmetry were confirmed by inspection of the axial oscillation photographs. The space group *Pcab* was determined uniquely based on the systematic extinctions occurring at $h = 2n + 1$ for $h0l$, $k = 2n + 1$ for $hk0$, and $l = 2n + 1$ for $0kl$. No absorption correction was deemed necessary.

The structure was solved by direct methods using MULTAN 80.[15] The *E* map corresponding to the largest combined figure of merit contained all the positions for non-hydrogen atoms. The non-hydrogen atoms were refined with anisotropic thermal parameters. Parameters for hydrogen atoms, however, were not varied. Instead, hydrogen atoms were placed at ideal positions with a C–H distance of 1.0 Å (B = 5–7 Å), depending on the size of the thermal motion of the corresponding C atom). In the final stage of the refinement, the weights were readjusted every three cycles of refinement in order to reduce the systematic variation of $\langle\omega(|F_o| - |F_c|)^2\rangle$ with $|F_o|$ and $(\sin\theta)/\lambda$. Refined positional parameters and anisotropic thermal parameters are given in Tables II and III, respectively. The structure factor table for (±)-**3** is available as supplementary material. Computer programs used in the analysis of the X-ray data have been cited elsewhere.[16]

X-ray Structure Determination of (−)-3. Parameters of the unit cell and information relevant to data collection appear in Table IV. Axial oscillation photographs indicated Laue symmetry $2/m$. Systematic ex-

Table I. Crystal Data and Relevant Diffraction Data for (±)-**3**

mol formula	$C_{11}H_{12}O_3$
recrystallizing solvent	ether–hexane
crystal system	orthohombic
space group	*Pcab*
a, Å	11.149 (3)
b, Å	16.065 (7)
c, Å	11.028 (4)
V, Å	1975 (1)
Z	8
ρ_{calcd}, g/cm^3, T, K	1.293, 298
crystal size, mm	0.2 × 0.5 × 0.7
μ, cm^{-1}	0.90
λ, Å (graphite-monochromated)	0.71069
diffractometer	Syntex $P2_1$
ω-step scan mode	3–30°/min
scan width, deg	1.0
background	same time as the peak scan
$2\theta_{max}$, deg	45
octants measured	hkl; $-h,k,-l$
crystal decay	linear 4.5% loss at end
no. of measd reflcns	3020
no. of obsd reflcns, ($I > 0$)	2165
no. of unique reflcns	444 ($I \geq 3\sigma_I$)
R, R_w,[a] %	6.4, 6.7

[a] $R \equiv \sum||F_o| - |F_c||/\sum|F_o|$. $R_w \equiv [\sum\omega(|F_o| - |F_c|)^2/\sum\omega|F_o|^2]^{1/2}$, initially $\omega = 1/\sigma_F^2$, readjusted slightly in the latter stages of refinement to minimize systematic errors. The function minimized was $\sum\omega(|F_o| - |F_c|)^2$.

(8) Boger, D. L.; Panek, J. S. *J. Org. Chem.* **1981**, *46*, 1208.
(9) Mori, K.; Ikunaka, M. *Tetrahedron* **1984**, *40*, 3471.
(10) Hayashi, H.; Nakanishi, K.; Brandon, C.; Marmur, J. *J. Am. Chem. Soc.* **1973**, *95*, 8749.
(11) Hanessian, S.; Ugolini, A., Dube, D.; Glamyan, A. *Can. J. Chem.* **1984**, *62*, 2146.
(12) Hungerbuhler, E.; Seebach, D.; Wasmuth, D. *Helv. Chim. Acta* **1981**, *64*, 1467.
(13) Yokoyama, Y.; Hall, H. K., Jr. *Macromolecules* **1980**, *13*, 252.
(14) Crank, G.; Eastwood, F. W. *Aust. J. Chem.* 1964, *17*, 1385.
(15) Main, P.; Fiske, S. J.; Hull, S. E.; Lessinger, L.; Germain, G.; Declerq, J.-P.; Woolfson, M. M. *MULTAN80—A System of Computer Programs for the Automatic Solution of Crystal Structures from X-ray Diffraction Data*; University of York: York, England, 1980.
(16) Kim, H. P.; Kim, S.; Jacobson, R. A.; Angelici, R. J. *J. Am. Chem. Soc.* **1986**, *108*, 5154. Non-hydrogen atomic scattering factors were those from: *International Tables for X-Ray Crystallography*; Kynoch: Birmingham, England, 1974; Vol. IV, Table 2.2A, pp 72–146. Hydrogen scattering factors were those of: Stewart, R. J.; Davidson, E. R.; Simpson, W. T. *J. Chem. Phys.* **1965**, *42*, 3175.

Table II. Positional Parameters[a] ($\times 10^4$) for (±)-3

atom	x	y	z	U_{eq}[b]
O7	−1291 (8)	506 (6)	1617 (8)	116 (4)
O1	−1156 (8)	956 (4)	3490 (8)	104 (4)
O5	203 (6)	70 (5)	2774 (9)	122 (4)
C9	275 (9)	1474 (6)	2130 (10)	52 (4)
C10	246 (9)	1734 (7)	950 (10)	68 (5)
C11	990 (10)	2381 (9)	570 (10)	105 (7)
C12	1720 (10)	2768 (7)	1360 (20)	97 (7)
C13	1754 (9)	2524 (8)	2570 (10)	90 (6)
C14	1018 (9)	1871 (7)	2952 (9)	62 (4)
C8	−458 (9)	736 (8)	2550 (10)	58 (5)
C4	−730 (20)	−640 (9)	2730 (10)	112 (8)
C6	−1460 (10)	−352 (8)	1660 (10)	129 (7)
C2	−1900 (10)	336 (9)	3950 (10)	139 (8)
C3	−1330 (20)	−510 (9)	3840 (10)	143 (9)
H19	−440	−1250	2450	63
H22	−320	1430	370	89
H23	940	2560	−360	89
H24	2280	3230	1030	89
H25	2310	2830	3170	89
H26	1030	1700	3870	89
H21	−2420	−470	1760	89
H20	−1290	−630	850	89
H15	−2230	440	4800	89
H16	−2710	280	3420	89
H17	−1870	−990	4110	89
H18	−640	−510	4530	89

[a] The estimated standard deviations in the parentheses are for the last significant digits. [b] $U_{eq} \equiv (10^3/3) \sum U_{ij} \vec{a}_i^* \cdot \vec{a}_j^* a_i a_j$, where the temperature factors are defined as $\exp(-2\pi^2 \sum h_i h_j a_i^* a_j^* U_{ij})$.

tinctions occurring at $k = 2n + 1$ for the $0k0$ reflections fixed the space group unambiguously as $P2_1$. Unit cell parameters derived from a least-squares calculation based on 15 intense reflections whose 2θ angles fell in the range of 30–35°. A single standard reflection monitored periodically throughout data collection indicated no appreciable decay. Since the most electron-dense atom in the crystal is oxygen, the data were not corrected for absorption of X-rays.

The structure was solved by direct methods using MULTAN 80.[15] The electron density map corresponding to the largest combined figure of merit revealed all non-hydrogen atoms. Difference electron density maps indicated clearly the locations of hydrogen atoms.

Four refined models differing only in their degree of geometric optimization were generated from the crystallographic data. Positional parameters for model 1 are listed in Table V. Model 1 derives from an unrestrained refinement using the anisotropic thermal parameters for non-hydrogen atoms (Table VI). Thermal parameters for hydrogen atoms were not refined. Instead, the thermal parameter of a given hydrogen was assigned the isotropic-equivalent value (i.e., the U_{eq} values in Table V) of the non-hydrogen atom to which it was linked. A similar procedure was carried out for model 2. It should be noted that values of U_{eq} of Table V for hydrogen atoms are only approximately equal to the values of U_{eq} of the corresponding non-hydrogen atoms in models 1 and 2, respectively. Shifts applied to the thermal parameters of non-hydrogen atoms were not applied to the thermal parameters of hydrogen atoms. Thus, after a cycle of refinement, the thermal parameters of a hydrogen atom and the corresponding non-hydrogen atom are only equal to within 1 standard deviation. The residual minimized in the least-squares refinement of model 1 was $\sum w(F_o - F_c)^2$, where w is the weighting factor $1/\sigma^2$. Refinement of model 1 made use of the program ALLS.[17] Models 2–4 differ from model 1 in that geometric restraints were applied to bond lengths, bond angles, and thermal parameters[18,19] with the program RESLSQ.[20] Ideal bond lengths used in the refinement appear in Table VII. The root-mean-square deviations from ideal bond lengths for models 2–4 were 0.032, 0.007, and 0.003 Å, respectively. As in the unrestrained model (model 1), non-hydrogen atoms of models 2–4 were refined anisotropically; the thermal parameters of hydrogen atoms were assigned the isotropic-equivalent values (U_{eq}) of the appropriate non-hydrogen atom. Structure factors for (−)-3, tables of positional and thermal parameters for models 2–4, and a complete list of bond lengths and bond angles are available as supplementary material.

Theoretical Methods. Intrinsic molar rotations at the sodium D line (5893 Å) were calculated from the dipole interaction theory as described elsewhere.[3] The calculation requires the coordinates and polarizability of each atom or group of atoms chosen as an interacting unit in the molecule. For the saturated moieties we have used the isotropic atom polarizabilities found previously:[7] C, 0.878; H, 0.135; O, 0.465 Å^3. The C_6 ring of the phenyl group was regarded as a single unit with an anisotropic polarizability located at the ring center, having components 7.069 Å^3 along the two principal axes in the plane of the ring and 6.989 Å^3 perpendicular to the plane of the ring. This treatment of the phenyl group, along with the assignment of isotropic polarizabilities of 0.135 Å^3 to the phenyl ring hydrogens, was found to give better overall agreement between calculated and observed polarizabilities and anisotropies of benzenes and methylbenzenes than an isotropic atom treatment of the ring carbons.[21] The accuracy of this polarizability is not a critical factor in the present work, since the calculated rotations are relatively insensitive to the phenyl polarizability.

Atomic coordinates of the phenyl ortho ester **3** were those found from the crystal structure of the pure enantiomer (−)-**3**. For **1** and **2**, the bicyclic moiety was taken to have the same structure as was found for (−)-**3**. The bond lengths[22] used for the bridgehead carbon substituent in **1** and **2** were C–H 1.095 Å and C–C 1.54 Å. Tetrahedral bond angles were assigned in the CH_3 substituent of **2**, and the group was placed in a staggered conformation relative to the three C–O (bridgehead) bonds. (Calculated optical rotations showed a change of less than 1% when the eclipsed conformation was assumed.) Optical rotations were calculated for each level of geometric restraint of the structural models derived from the diffraction data for (−)-**3**.

Optical Activity Measurements on Single Crystals of (±)-3. HPLC separation was performed on a 25 × 0.46 cm, 5-μm Hypersil ODS column (Alltech), using HPLC-grade methanol as eluent (Fisher Scientific). HPLC studies of optical activity allow sensitivities about 3 orders of magnitude better than static measurements.[23,24] The solvent was chosen to have an elution strength that allows **3** to be well separated from any potential impurities, despite the fact that slight decomposition of **3** occurs if long residence times are involved. A UV absorbance detector (Altex, Model 153) was used in series before the optical activity flow cell. A flow rate of 0.47 mL/min was provided by a syringe pump (Isco, Model LC2600). Injections were made through a conventional injection valve (Rheodyne, Model 7010) with a 10-mL loop. The arrangement of a laser-based optical activity detector (OAD) for LC has been reported earlier.[23,24] The noise level of the system is equivalent to 10 μdeg of rotation. The area under each peak was determined and then normalized against the signal obtained from the DC Faraday rotator[23] for each chromatographic trial. The specific rotation of the compound can be calculated from the peak area, the amount injected, and the flow rate. The specific rotation is obtained by using the relationship $[\alpha] = \alpha/cl$ where α is the actual rotation measured, c is the concentration in grams of solute per milliliter of solution, and l is the path length in decimeters. Samples of (−)-**3**, (±)-**3**, and single crystals of (±)-**3** were used in the analysis. Solutions of the samples were prepared in HPLC-grade methanol and subjected to HPLC immediately to minimize solvolysis. Sample concentrations ranged from 0.5 to 0.15 mg/mL. The racemic mixture was used to determine appropriate chromatographic conditions (UV detection). Since the racemic mixture should produce no OAD signal, it was used to determine the upper limit in concentration that did not produce an appreciable base line disturbance caused by a refractive index change upon elution of the sample. A small disturbance was observed in the concentration range used, but its shape is indicative of a refractive index change and not optical activity. The chromatograms for the optically active compound served as an indication of the magnitude of optical activity response to expect when an optically active sample is present, as well as to determine an appropriate range of concentrations for the OAD. For the analysis of the single crystals of the racemic preparation, one crystal was weighed and then dissolved in methanol (1–3 mL) to achieve a concentration similar to that in the previous experiment.

Results

Synthesis. Racemic **1** has been realized previously in 2.3% yield from the uncatalyzed reaction of 1,2,4-butanetriol and triethyl

(17) Lapp, R. L.; Jacobson, R. A. *ALLS*; U.S. Department of Energy Report IS-4708, Iowa State University: Ames, IA, 1979.
(18) Konnert, J. (1976) *Acta Crystallogr., Sect. A: Cryst. Phys. Diffr. Theor. Gen. Crystallogr.* **1976**, *A32*, 614.
(19) Konnert, J.; Hendrickson, W. A. *Acta Crystallogr., Sect. A: Cryst. Phys. Diffr. Theor. Gen. Crystallogr.* **1980**, *A36*, 344.
(20) Flippen-Anderson, J. L.; Gilardi, R.; Konnert, J. H. *NRL Memorandum Report 5042, Restrained Least Squares Program (RESLSQ) Users Manual*; Naval Research Laboratory: Washington, DC, 1983.
(21) Caldwell, J. W.; Applequist, J., unpublished results.
(22) Pauling, L. *The Nature of the Chemical Bond*, 3rd ed.; Cornell University: Ithaca, 1960.
(23) Yeung, E. S.; Steenhoek, L. E.; Woodruff, S. D.; Kuo, J. C. *Anal. Chem.* **1980**, *52*, 1399.
(24) Kuo, J. C.; Yeung, E. S. *J. Chromatogr.* **1982**, *253*, 199.

Table III. Anisotropic Thermal Parameters[a] ($\times 10^3$) for (±)-**3**

atom	U_{11}	U_{22}	U_{33}	U_{23}	U_{13}	U_{12}	atom	U_{11}	U_{22}	U_{33}	U_{23}	U_{13}	U_{12}
O7	132 (8)	107 (7)	109 (7)	30 (7)	−33 (7)	−56 (6)	C13	66 (9)	68 (8)	140 (10)	3 (10)	−3 (10)	−30 (8)
O1	113 (8)	70 (5)	129 (8)	−8 (6)	75 (7)	−15 (5)	C14	56 (8)	78 (8)	50 (7)	0 (7)	−9 (6)	0 (7)
O5	59 (6)	61 (5)	250 (10)	49 (7)	14 (7)	6 (5)	C8	38 (7)	64 (8)	73 (9)	−1 (7)	6 (9)	−5 (7)
C9	49 (8)	50 (6)	57 (8)	20 (6)	−1 (6)	13 (6)	C4	170 (20)	100 (10)	70 (10)	12 (9)	−10 (10)	30 (10)
C10	58 (8)	89 (8)	59 (8)	26 (8)	−9 (6)	−11 (7)	C6	180 (20)	80 (10)	120 (10)	3 (10)	−50 (10)	−50 (10)
C11	90 (10)	110 (10)	120 (10)	40 (10)	20 (10)	−11 (9)	C2	170 (20)	90 (10)	160 (10)	−10 (10)	100 (10)	−50 (10)
C12	80 (10)	72 (9)	140 (20)	40 (10)	20 (10)	0 (7)	C3	260 (20)	100 (10)	70 (10)	50 (10)	−20 (10)	−30 (10)

[a] Estimated standard deviations are in parentheses. The anisotropic temperature factors are defined as $\exp(-2\pi^2\sum h_i h_j a_i^* a_j^* U_{ij})$.

Table IV. Crystal Data and Relevant Diffraction Data for (−)-**3**

mol formula	$C_{11}H_{12}O_3$
recrystallizing solvent	ether–hexane
crystal system	monoclinic
space group	$P2_1$
a, Å	7.8520 (9)
b, Å	10.493 (1)
c, Å	6.1048 (6)
β, °	107.02 (1)
V, Å^3	481.35 (9)
Z	2
ρ_{calcd}, g/cm^3	1.326
crystal size, mm	0.4 × 0.6 × 1.0
μ, cm^{-1}	0.92
λ, Å	0.71069
diffractometer	Syntex $P2_1$
ω-step scan mode	3–30 °/min
scan width, deg	1.0
background	same time as the peak scan
$2\theta_{max}$, deg	55
octants measured	hkl; $-h,k,l$
no. of measd reflcns	1255[a]
no. of obsd reflcns ($I > 0$)	1151
no. of used reflcns	1151
R (models 1–4)[b] %	6.12, 6.12, 6.79, 9.57
R_w (models 1–4),[c] %	4.53, 4.50, 5.48, 8.74
S (models 1–4)[d]	1.60, 1.58, 2.34, 5.96
max shift/error for models 1–4	0.85, 0.75, 0.83, 0.92

[a] Extinct reflections not included. [b] $R \equiv (\sum||F_o| - |F_c||)/\sum|F_o|)$. Models 1–4 are described in the text. [c] $R_w \equiv [[\sum\omega(|F_o| - |F_c|)^2]/[\sum\omega|F_o|^2]]^{1/2}$, where $\omega = 1/\sigma_F^2$. [d] $S \equiv [[\sum(F_o - F_c)^2]/N]^{1/2}$.

orthoformate.[14] More recently, the yield of this reaction was improved to 70.9% by removing (±)-**1** from the *p*-toluenesulfonic acid catalyzed equilibrium mixture.[13] Although our HCl-catalyzed synthesis of (±)-**1** and (−)-**1** led to considerably lower yields (37 and 13.5%, respectively), the yields of the new methyl analogue (±)-**2** and (−)-**2** (74 and 63%, respectively) were comparable to the yield reported earlier for (±)-**1**, and the yields of the new phenyl derivative (±)-**3** and (−)-**3** (35 and 39%, respectively) were quite reasonable. Of the three enantiomerically pure compounds, only (−)-**3** gave crystals suitable for X-ray diffraction experiments.

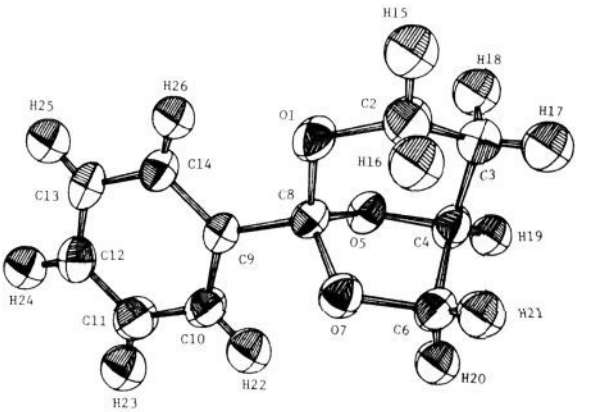

Figure 1. ORTEP drawing of the crystallographically determined structure of (−)-**3**.

Structure Refinements. The ORTEP drawing of (−)-**3** is shown in Figure 1. Crystals of (±)-**3** diffract to lower resolution than those of (−)-**3**. The difference in diffraction properties of the two crystal forms manifests itself in the level of uncertainty associated with refined parameters as well as the absolute magnitude of thermal values. Thus, crystals of (±)-**3** (lower resolution form) yield less accurate parameters and larger thermal values than those from crystals of (−)-**3**. The less efficient packing engendered by the presence of both enantiomers in crystals of (±)-**3** is also evident

Table V. Positional Parameters[a] ($\times 10^4$) for Model 1 of (−)-**3**

atom	x	y	z	U_{eq}[b]	atom	x	y	z	U_{eq}[b]
O1	265 (3)	3773 (0)	2712 (4)	51	C14	3103 (4)	2212 (4)	4741 (5)	45
O5	405 (2)	2833 (3)	−635 (3)	41	H15	−2050 (50)	4630 (50)	2590 (80)	58
O7	1851 (2)	4673 (3)	458 (4)	44	H16	−780 (60)	5400 (50)	1560 (90)	58
C2	−1234 (5)	4571 (5)	1575 (7)	59	H17	−2940 (50)	4820 (50)	−1800 (80)	55
C3	−2131 (4)	4138 (5)	−857 (7)	54	H18	−2860 (50)	3270 (50)	−860 (80)	55
C4	−711 (4)	3817 (4)	−2003 (6)	43	H19	−1260 (50)	3460 (40)	−3610 (80)	45
C6	647 (7)	4857 (4)	−1810 (6)	47	H20	1320 (50)	4790 (40)	−2880 (70)	47
C8	1360 (4)	3519 (3)	1322 (5)	37	H21	80 (50)	5670 (50)	−1970 (80)	47
C9	2973 (4)	2789 (4)	2642 (5)	39	H22	4270 (50)	3050 (50)	220 (80)	56
C10	4349 (4)	2633 (4)	1688 (6)	58	H23	6870 (60)	1850 (50)	2190 (80)	65
C11	5817 (5)	1910 (5)	2771 (7)	67	H24	7070 (60)	840 (50)	5800 (80)	57
C12	5949 (5)	1340 (4)	4866 (6)	55	H25	4600 (50)	1010 (40)	7210 (80)	54
C13	4585 (5)	1492 (4)	5839 (6)	52	H26	2130 (50)	2360 (40)	5280 (70)	45

[a] Estimated standard deviations are in parentheses. [b] $U_{eq} = (10^3/3)\sum U_{ij}\vec{a}_i^*\cdot\vec{a}_j^* a_i a_j$.

Table VI. Anisotropic Thermal Parameters ($\times 10^3$) for Model 1 of (−)-**3**

atom	U_{11}	U_{22}	U_{33}	U_{23}	U_{13}	U_{12}	atom	U_{11}	U_{22}	U_{33}	U_{23}	U_{13}	U_{12}
O1	54 (1)	63 (1)	36 (1)	18 (1)	20 (1)	7 (1)	C9	44 (1)	40 (1)	33 (1)	1 (1)	9 (1)	3 (1)
O5	53 (1)	36 (1)	35 (1)	−3 (1)	9 (1)	−1 (1)	C10	55 (2)	70 (2)	49 (2)	12 (2)	24 (2)	18 (2)
O7	50 (1)	39 (1)	41 (1)	−5 (1)	10 (1)	2 (1)	C10	55 (2)	70 (2)	49 (2)	12 (2)	24 (2)	18 (2)
C2	55 (2)	68 (2)	55 (2)	22 (2)	25 (2)	12 (2)	C11	56 (2)	77 (2)	68 (2)	19 (2)	27 (2)	21 (2)
C3	45 (2)	65 (2)	53 (2)	1 (2)	13 (2)	15 (2)	C12	53 (2)	59 (2)	54 (2)	10 (2)	7 (2)	12 (2)
C4	48 (1)	47 (2)	33 (2)	−3 (1)	4 (1)	5 (1)	C13	64 (2)	60 (2)	34 (2)	5 (2)	6 (2)	7 (2)
C6	52 (2)	48 (2)	39 (2)	−1 (2)	12 (1)	9 (2)	C14	52 (2)	50 (2)	33 (2)	2 (1)	11 (1)	2 (1)
C8	43 (1)	40 (2)	29 (1)	0 (1)	12 (1)	0 (1)							

Table VII. Ideal Bond Lengths (Å) and Ranges in Observed Bond Lengths for Models of (±)-3 and (−)-3

bond	ideal	(±)-3	model 1	model 2	model 3	model 4
C–O	1.42	1.32–1.55	1.400–1.451	1.401–1.453	1.408–1.435	1.418–1.428
C–C aliphatic	1.54	1.41–1.51	1.499–1.518	1.500–1.518	1.524–1.535	1.536–1.540
C–C aromatic	1.39	1.35–1.40	1.377–1.393	1.381–1.392	1.386–1.389	1.389–1.390
C–H aliphatic	1.095	1.0–1.1	0.94–1.08	1.03–1.09	1.08–1.10	1.09–1.10
C–H aromatic	1.084	1.0	0.93–1.04	1.02–1.06	1.08	1.08

Table VIII. Intrinsic Molar Rotations (deg cm²/dmol) of (−)-1, (−)-2, and (−)-3 from Geometrically Restrained Models of (−)-3

compd	model 2	model 3	model 4	exptl
1	−4809	−711	−404	−145.2
2	−5372	−829	−508	−120.5
3	−5063	−769	−427	−121.5

in its smaller density (1.293 g/cm³) compared with that of (−)-3 (1.326 g/cm³). Since calculated optical rotations vary strongly with bond lengths, only the more accurate models 1–4, based on crystals of (−)-3, were used in calculations of optical rotations.

Geometric optimization of the structural parameters of model 1, as described in the Experimental Section, gave rise to model 2, which accounts for the X-ray diffraction data as well as does the unrestrained model (model 1). Whereas the geometric restraints for model 3 give rise to a structure that is only marginally poorer in accounting for the X-ray diffraction data, the high degree of geometric optimization associated with model 4 is clearly not substantiated by the diffraction data since the statistics (R, R_w, and S of Table IV) are significantly higher for model 4 than for models 1 and 2. In general, restraints have the greatest effect on the positions of hydrogen atoms. The electron density associated with a hydrogen atom lies in the covalent bond between the proton and the nucleus of the non-hydrogen atom. An unrestrained refinement, which places the atomic nucleus within the region of peak electron density, produces systematically short covalent bonds for hydrogen atoms. Because the electron density associated with a hydrogen atom is low and is therefore a weak determinant of the position of the proton, geometric restraints greatly influence the positions of hydrogen atoms but have relatively small effects on the locations of non-hydrogen atoms.

Molar Rotation Calculations. Table VIII lists the intrinsic molar rotations $[m]_D$ calculated for ortho esters **1–3** by using each of the three geometrically restrained models. Meaningful results could not be obtained for the unrestrained model (model 1), for reasons presented below. The calculated rotations agree in sign with the experimental values but are of considerably larger magnitude. However, the calculated rotations converge toward the experimental values with succeeding levels of geometric restraint (models 2, 3, and 4, in that order). The reasons for this behavior and for the discrepancies between theory and experiment will also be discussed.

A notable feature of both the theoretical and experimental rotations is that they are rather insensitive to the substituent at the bridgehead carbon. To test this idea further, calculations were carried out on **3** with the phenyl group rotated through various angles about the C8–C9 axis (Figure 1). For model 4, $[m]_D$ was found to vary over the range −417 to −535 deg cm²/dmol over the 0–360° torsion angle range. Thus, the conformation has no effect on the sign or order of magnitude of the rotation. In a further calculation, substitution of an isotropic polarizability of 7.00 Å³ for the C_6 ring (in place of the anisotropic polarizability adopted above) produced a negligible change in the calculated rotation of (−)-3. Thus, the rotation of (−)-3 appears to be only moderately sensitive to the polarizability of the phenyl group, and the provisional treatment of that group given here should not be a cause of the observed discrepancies.

The insensitivity of the rotation to the nature of the substituent on C8 may seem surprising since that carbon is chiral. Some insight into the origin of optical activity in these compounds can be gained by noting that the butane fragment C2–C3–C4–C6 is locked into a gauche conformation that is itself optically active. If we extract that fragment, with its hydrogens, from the structure of (−)-3 (model 4) and replace the oxygens with hydrogens (using 1.095 Å for the C–H bond lengths), we calculate an intrinsic molar rotation of −1312 deg cm²/dmol for this conformationally rigid butane fragment. This is of the same sign and order of magnitude as the rotations calculated for all three ortho esters, suggesting that interactions within the chiral butane fragment are largely responsible for the observed rotations.

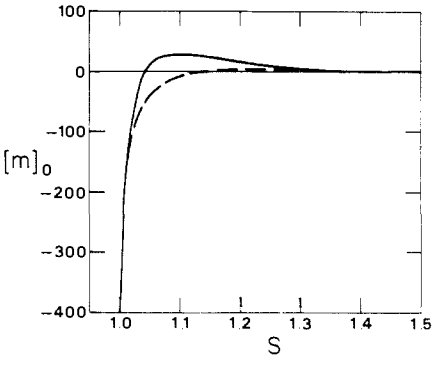

Figure 2. Intrinsic molar rotation (deg cm²/dmol) calculated for **3** (—) and **1** (- - -) as a function of scale factor S.

The trend in the calculated rotations toward the experimentally determined values with increasing level of geometric restraint most likely originates in the fact that the bond lengths are relatively small for the unrestrained model and tend to increase toward the target values with increasing restraint (see Table VII). The target bond lengths in the restrained refinements were those adopted for the model compounds on which the atom polarizabilities are based. The use of shorter bond lengths with the same polarizabilities tends to exaggerate the interactions among atoms, since these vary as the inverse cube of the interatomic distances in the dipole interaction model.[3]

Figure 2 shows the effect of interatomic distances on rotations in another way. Here the atom coordinates in (−)-**1** and (−)-**3** have been multiplied by a scale factor S in order to expand all the interatomic distances uniformly, and the calculated rotation is given as a function of S. At $S = 1.00$, the structures are those of model 4. The rotations are seen to be very sensitive to S near $S = 1$, so that a change in scale of less than 2% removes the discrepancy between theory and experiment described above. It is worth noting that the inverse-cube dependence of interactions on distances would result in a rotation that falls off as S^{-2}, if first-order (pairwise) interactions predominate, or as S^{-3n+1} if nth-order interactions predominate. The curves in Figure 2 near $S = 1$ vary as S^{-93} for **3** and S^{-37} for **1**. These dependencies show that interactions of high order are predominant in these molecules, though they do not suggest the predominance of any single order.

The predominance of high-order interactions means that the series expansion for the inverse of the interaction matrix **A** converges slowly.[25] This implies that **A** is not far from a singularity, i.e., a condition under which its determinant $|\mathbf{A}|$ vanishes. We can learn more about the proximity of a singularity by examining the eigenvalues of **A**. If an eigenvalue is zero, then **A** is singular. If an eigenvalue is negative, then the system is unstable, and the parameters used are physically unrealistic. If all eigenvalues are

(25) Applequist, J. *J. Chem. Phys.* **1973**, *58*, 4251.

Table IX. Lowest Eigenvalue of Interaction Matrix for Models of (−)-**3** at Various Levels of Geometric Constraint

model	lowest eigenvalue, Å^{-3}	model	lowest eigenvalue, Å^{-3}
1	−0.1309	3	0.0892
2	0.0381	4	0.1065

positive, the smallest value represents the smallest displacement of the inverse atom polarizabilities that would bring **A** to a singularity.[25] Table IX shows the lowest eigenvalues computed for **A** for each of the models for (−)-**3** considered in this study. The values are seen to increase from a negative quantity for the unrestrained model 1 through a range of positive values for restrained models. This trend is correlated with the trend in the calculated optical rotations. No optical rotation was obtained for model 1 because, according to the negative eigenvalue, the parameters of the system are unrealistic. The largest rotations were calculated for the model with the smallest positive eigenvalue, corresponding to the fact that the rotation tends toward infinity as a singularity is approached. As a point of reference, it may be noted that the lowest eigenvalue for CH_4 by the same theory is 0.476 Å^3, which is substantially larger than the values for (−)-**3**.

Optical Activity Measurements on Single Crystals of (±)-3. The X-ray diffraction studies revealed significant differences between the crystals of (±)-**3** and (−)-**3** but did not show directly whether the (±)-**3** single crystal is racemic or enantiomeric. To make this determination, optical activity measurements on the (±)-**3** single crystal in solution were carried out by a high-sensitivity HPLC method. Samples of (−)-**3** showed that concentrations below ~0.5 mg/mL were low enough to avoid false signals (caused by refractive index changes) that could be confused with optical activity. The optically active sample of (−)-**3** reinforced this observation, since concentrations above 0.3 mg/mL produce signals that could not be confused with a refractive index change. A shoulder on the peak was observed for the solutions prepared from the racemic preparation. In the optically active sample, the shoulder was a peak, accounting for approximately 30% of the total peak area. In samples of the single crystals the first peak was larger than the second. Specific rotation was calculated for the optically active sample. The average specific rotation from 13 chromatograms of (−)-**3** is −46 (14)°. If the results of the two peaks are calculated separately, the specific rotation for the first peak is −17 (4)° and that for the second peak is −65 (14)°. These results are consistent with the conclusion that the compound associated with the peak of smaller specific rotation is a methanolysis product. Calculation of the specific rotation of both peaks in the single-crystal samples of (±)-**3** yields an average value of −4 (6)°, indicating that the single crystals are racemic in composition, with the presence of a maximum of 9% excess of one enantiomer.

Discussion

Experiment shows that the ortho esters (−)-**1**–(−)-**3** derived from (*S*)-(−)-1,2,4-butanetriol are all levoratatory with approximately equal molar rotations. In these molecules the bridgehead ortho ester carbon has the *R* configuration while the primary chiral carbon of the butane moiety is *S*.

The surprisingly large thermal parameters for the (±)-**3** crystal form reflect appreciable packing disorder. The packing disorder could stem from the absence of intramolecular hydrogen bonds. However, crystals of (−)-**3** also lack intramolecular hydrogen bonds and yet exhibit good order. Any deviation from a racemic composition of **3** in the (±)-**3** crystal form would result in disorder, simply because the *Pcab* space group requires a 50:50 ratio of both enantiomers. Measurements of optical activity, however, indicate a racemic mixture in the crystal. Another source of packing disorder, and perhaps the most likely explanation of the disorder in crystals of (±)-**3**, stems from the statistical occupancy of specific crystal sites by the enantiomer of the wrong hand. The mismatch of enantiomer with crystal site could occur even in a racemic compound. A mismatching frequency of up to 20% would be difficult to detect as such in the electron density but could have a significant effect on the refinement parameters.

The signs of the rotations calculated from the dipole interaction theory are in agreement with the experimentally determined signs. The calculated magnitudes of the rotations are severalfold too large, but this appears to result from small differences between bond lengths found by X-ray diffraction for (−)-**3** and those assumed in the determination of atom polarizabilities from model compounds. The differences in bond lengths may be real, since the agreement between calculated and observed X-ray diffraction intensities is somewhat poorer when the structure is restrained to approach the selected target bond lengths on which the polarizabilities are based. If this is the case, then the discrepancies in the theoretical rotations would be due, at least in part, to the fact that the atom polarizabilities are not strictly transferable among molecules with different geometries for similar types of bonds.

The ability of the theory to give the correct sign of the rotation means that it does correctly relate the sign to the absolute configuration. Our theoretical model suggests that the sign is related primarily to the conformation of the butane fragment of the bicyclic structure. It should be noted, however, that the sign is not determined solely by the torsion angles of the butane group but is sensitive to small variations in other structural parameters. For example, Figure 2 shows that positive rotations are predicted when the structure is expanded by 5–10%. This observation would not seem to engender appreciable uncertainty in the sign predicted by theory in the three cases studied here, though it raises a problem that may arise generally in applications of the theory of optical rotation.

Addendum. A reviewer has suggested that the molar rotations be calculated on the basis of model 1 with the hydrogen atoms repositioned at idealized locations with C–H = 1.095 Å, arguing that this would cause no deterioration of the fit to the X-ray diffraction data, as does the restrained refinement procedure used here. The rotation so calculated for compound **3** is $[m]_D$ = −1449 deg cm^2/dmol. This shows that repositioning the hydrogen atoms alone does relieve most of the problem with the unrestrained structure, which otherwise did not yield a meaningful result, as noted above. However, the results in Table VIII show that repositioning of the heavy atoms by restrained refinement has a greater effect. When the hydrogens are similarly repositioned to C–H = 1.095 Å in model 2, which fits the X-ray diffraction data as well as model 1, the calculated rotation is $[m]_D$ = −1663 deg cm^2/dmol, in contrast with the value −5063 deg cm^2/dmol for the unshifted hydrogens (Table VIII). Again, this shows that the error in the latter value results in part from short C–H distances. The reviewer's suggestion arises from a concern that our restrained refinements simply "fudge" the data in order to match theory with observation. Models 3 and 4 do clearly represent structures that fit the diffraction data less well than models 1 and 2 and must therefore be regarded as being further from the true structure. However, their inclusion in this study serves a useful purpose: They show that the theory is capable of producing molar rotations comparable to experiment only when the internuclear distances approach those of the model compounds from which the atom polarizabilities were derived. This understanding of the source of the discrepancy should be useful in guiding further studies of this type. For example, it may prove possible to correct atom polarizabilities for changes in bond lengths, using polarizability parameters similar to those obtained from a study of Raman scattering intensities.[26] If this were done, it might be possible to calculate better rotations from unrestrained X-ray structures.

Acknowledgment. J.G.V. acknowledges the National Science Foundation and the donors of the Petroleum Research Fund, administered by the American Chemical Society, for partial support of this research. J.A. acknowledges support through a research grant from the National Institutes of General Medical Sciences (GM13684). The research of S.-S.K., R.A.J., B.H.R., and E.S.Y. was supported by the U.S. Department of Energy, Office of Basic Energy Sciences, Materials Science Division and

(26) Applequist, J.; Quicksall, C. O. *J. Chem. Phys.* **1977**, *66*, 3455.

Chemical Sciences Division. R.H. acknowledges support by the donors of the Petroleum Research Fund, administered by the American Chemical Society, and support from the National Institutes of General Medical Sciences (GM33828). We also thank Pat Cyr for experimental assistance.

Supplementary Material Available: Tables of positional and anisotropic thermal parameters, bond lengths, and bond angles (14 pages); tables of calculated and observed structure factors (7 pages). Ordering information is given on any current masthead page.

Effects of Solvents, Axial Ligation, and Radical Cation Formation on the V=O Stretching Raman Frequency in Vanadyl Porphyrins: Implications for Peroxidase Intermediates

Y. Oliver Su,† Roman S. Czernuszewicz, Lisa A. Miller, and Thomas G. Spiro*

Contribution from the Department of Chemistry, Princeton University, Princeton, New Jersey 08544. *Received August 27, 1987*

Abstract: The systematics of the V=O stretching frequency in vanadyl porphyrins are investigated with resonance Raman (RR) spectroscopy. For a series of solvents the frequency decreases with increasing solvent acceptor number, consistent with solvent-induced polarization of the V-O bond. Variations in the solvent dependence are seen for different porphyrins, reflecting different polarization effects of the peripheral substituents. In coordinating solvents a second V-O stretching band, at lower frequency, arises from six-coordinate species. The downshift in ν_{V-O} upon ligation increases with increasing donor strength of the ligand. It is larger for imidazolate than imidazole, and it is especially large for hydroxide; the hydroxide effect is attributed to $OH^- \rightarrow V^{IV}$ π-donation, competing with the oxo ligand for acceptor d orbitals. The RR spectrum of $(VO)OEP^{\cdot+}$ produced by electrochemical oxidation shows porphyrin skeletal mode frequency shifts similar to those seen for other OEP π-cation radicals. The V-O stretching frequency increases 15 cm^{-1} relative to (VO)OEP. These findings are discussed in relation to recent RR data on ferryl porphyrins and ferryl species in heme proteins. Differences among these species can be accounted for on the basis of proximal and distal effects.

Oxometal complexes are implicated in oxygen activation by heme proteins. The peroxidase intermediates, compounds I and II, are known to contain ferryl heme.[1-3] This species is also believed to participate in the mechanism of catalytic oxidation and hydroxylation by cytochrome P_{450} enzymes.[4,5] Considerable progress has been made in probing the nature of the Fe-O bond via EXAFS[6-9] and resonance Raman (RR) spectroscopies.[10-18] RR studies of horseradish peroxidase (HRP) compound II[10,13,16,17] and the ES complex of cytochrome *c* peroxidase (CCP)[14,18] reveal a bond of moderate strength. In HRP the O atom is H-bonded to a titratable distal residue, probably histidine. In order to evaluate the resonance Raman evidence it is desirable to examine reference complexes with systematic variation of both distal and proximal interactions. In addition, since compound I of peroxidases contains a ferryl porphyrin π-cation radical, it is of interest to anticipate the effect on the Fe=O bond of ring oxidation.

Isolated ferryl porphyrins have yielded informative RR spectra[19-22] but are of limited stability and do not readily lend themselves to systematic studies. Accordingly we have turned to vanadyl porphyrin, which has a stable V-O bond,[23] and can be examined in a variety of environments. In this study we evaluate solvent effects, including H-bonding, axial ligand interactions, and radical cation formation on the stretching frequency of the V-O bond, as monitored by RR spectroscopy. These frequency variations throw light on the available data for ferryl hemes and allow evaluation of the chemical interactions in the binding pocket of ferryl heme-containing proteins.

Experimental Section

Vanadyl complexes of octaethylporphyrin (OEP), tetraphenylporphyrin (TPP), and tetrakis(methylpyridinium)porphyrin (TMPyP) were purchased from Mid Centry Chemicals (Posen, IL). They were dissolved in spectral grade solvents, and their UV-vis spectra were checked. When necessary they were chromatographed on alumina (A

* Author to whom correspondence should be addressed.
† Present address: Department of Chemistry, National Taiwan University, Taipei, Taiwan, Republic of China.

(1) Critchlow, J. E.; Dunford, H. B. *J. Biol. Chem.* **1972**, *247*, 3714-3725.
(2) Roberts, J. E.; Hoffman, B. H.; Rutter, R.; Hager, L. P. *J. Am. Chem. Soc.* **1981**, *103*, 7654-7656.
(3) LaMar, G. N.; DeRopp, J. S.; Latos-Grazynsky, L.; Balch, A. L.; Johnson, R. B.; Smith, K. M.; Parish, D. W.; Chen, R. *J. Am. Chem. Soc.* **1983**, *105*, 782-787.
(4) Griffin, B. W.; Peterson, J. A.; Estabrook, R. W. In *Porphyrins*; Dolphin, D., Ed.; Academic: New York, 1979; Vol. 7, p 333.
(5) White, R. E.; Coon, M. J. *Annu. Rev. Biochem.* **1980**, *49*, 315-356.
(6) Penner-Hahn, J. E.; McMurry, T. J.; Renner, M.; Latos-Grazynsky, L.; Eble, A. S.; Davis, I. M.; Balch, A. L.; Groves, J. T.; Dawson, J. H.; Hodgson, K. O. *J. Biol. Chem.* **1983**, *258*, 12761-12764.
(7) Penner-Hahn, J. E.; Eble, K. S.; McMurry, T. J.; Renner, M.; Balch, A. L.; Groves, J. T.; Dawson, J. H.; Hodgson, K. O. *J. Am. Chem. Soc.* **1986**, *108*, 7819-7825.
(8) Chance, M.; Powers, L.; Kumar, C.; Chance, B. *Biochemistry* **1986**, *25*, 1259-1265.
(9) Chance, M.; Powers, L.; Poulos, T.; Chance, B. *Biochemistry* **1986**, *25*, 1266-1270.
(10) Terner, J.; Sitter, A. J.; Reczek, C. M. *Biochim. Biophys. Acta* **1985**, *828*, 73-80.
(11) Sitter, A. J.; Reczek, C. M.; Terner, J. *Biochim. Biophys. Acta* **1985**, *828*, 229-235.
(12) Sitter, A. J.; Reczek, C. M.; Terner, J. *J. Biol. Chem.* **1985**, *260*, 7515-7520.
(13) Sitter, A. J.; Reczek, C. M.; Terner, J. *J. Biol. Chem.* **1986**, *261*, 8638-8642.
(14) Sitter, A. J.; Reczek, C. M.; Terner, J., manuscript in preparation.
(15) Hashimoto, S.; Tatsuno, Y.; Kitagawa, T. *Proc. Jpn. Acad. Ser. B. Phys. Biol. Sci.* **1984**, *60*, 345-348.
(16) Hashimoto, S.; Tatsuno, Y.; Kitagawa, T. *Proc. Natl. Acad. Sci. U.S.A.* **1986**, *83*, 2417-2421.
(17) Hashimoto, S.; Teraoka, J.; Inubushi, T.; Yonetani, T.; Kitagawa, T. *J. Biol. Chem.* **1986**, *261*, 11110-11118.
(18) Makino, R.; Uno, T.; Nishimura, Y.; Iizuka, T.; Tsuboi, M.; Ishimura, Y. *J. Biol. Chem.* **1986**, *261*, 8376-8382.
(19) (a) Bajdor, K.; Nakamoto, K. *J. Am. Chem. Soc.* **1984**, *106*, 3045. (b) Proniewicz, J. M.; Bajdor, K.; Nakamoto, K. *J. Phys. Chem.* **1986**, *90*, 1760-1766.

0002-7863/88/1510-4150$01.50/0